ACADEMIA ROMÂNĂ
*Revue Roumaine de Chimie*
http://web.icf.ro/rrch/

*Rev. Roum. Chim.*,
**2017**, *62*(11), 857-863

# ELECTRO-SYNTHESIS AND LUMINESCENCE PROPERTIES OF $Zn_2SiO_4$:Mn NANO-PARTICLES

Malektaj KHAZAEI and Ali PARSA*

Department of Chemistry, College of Science, Yadegar -e- Imam Khomeini (RAH) Shahre Rey Branch, Islamic Azad University, Tehran, Iran

*Received January 14, 2017*

This study is the first such research into the successful electrosynthesis of $Zn_2SiO_4$:$Mn^{2+}$ phosphor by sequential cyclic voltammetry and potansiostate methods in the potential range of -0.8 to 0.0 V and 0.9 V constant potential, respectively. Oxidative electrosynthesis of $SiO_2$ was performed using 10 mL solution containing 0.1 M $(NH_4)_2SiF_6$ and 0.5 M potassium chloride as supporting electrolyte on composite 2B pencil graphite. $Zn_2SiO_4$:$Mn^{2+}$ nanocomposite electrosynthesis was then accomplished using immersion of the modified electrode with $SiO_2$ in the zinc nitrate and manganese nitrate, including potassium fluoride and potassium chloride, for five minutes in a 0.9 V constant potential. By varying the concentration of manganese nitrate, nanocomposites with different luminescence properties were obtained. Mn-doped $Zn_2SiO_4$ nanoparticles with suitable optical properties were used in the fabrication of cement plasts (artificial stones) with properties of luminescence. The nanocomposite phosphors have been characterized using XRD, SEM, EDX, FT-IR and photo-luminescence spectroscopic techniques.


## INTRODUCTION

Phosphorus is the main element of luminescence projectors. It is also used in compact fluorescent lamp (CFLs), medical sciences, detectors, communications, laser and electronics. Hence, the expansion of these industries depends on the expansion of studies in the field of phosphorous producing.[1–5] However, the rare metal compounds of the earth that contain phosphorus have some advantages with regard to semiconductor phosphorus due to its higher colour purity and shorter response time.[6, 7]

In the process of luminescence, a few atoms (which are usually impure atoms or doped atoms) are stimulated, causing the radiation. These types of atoms are called radiation centers. In this process, the electron of the capacity layer is stimulated and then transferred to a higher circuit, and then a photon is dispatched and returned to the base circuit. Ultimately, all the dispatched photons produce the phenomenon of luminescence.[8, 9]

The capacity of most phosphors, including earth metal compounds, is used because of the small energy gap and easy to stimulate electron layer. Zinc—widely used as a host in phosphors—is one of the luminescence compounds considered an

* Corresponding author: aliparsa@iausr.ac.ir or iausr.parsa@yahoo.com (Ali Parsa),Tel.: +98 21 55229208 ;Fax: +98 21 55229297

earth metal. It was the topic for many researches.[10-13] Zinc is not used alone – impurities such as sulphur are used in it.[14, 15]

Green phosphor nanoparticles of $Zn_2SiO_4:Mn^{2+}$ have been widely used in plasma display panels (PDP), cathode ray tubes (CRT), and thin film electroluminescent (EL) devices, thanks to its high luminescent efficiency.[16–19]

In this paper, $Zn_2SiO_4:Mn^{2+}$ nanocomposites were prepared by the electrochemical method. Cyclic voltammetry is a new technique capable of producing nanocomposites with high-density crystallized nanoparticles. These can be directly deposited onto the composite graphite surface. We also clarified the influence of variations in the concentration of manganese nitrate on the properties of luminescence of $Zn_2SiO_4:Mn^{2+}$.

## EXPERIMENTAL

### Materials

Ammonium hexafluorosilicate, potassium chloride and potassium fluoride (Sigma Chemicals, USA) were used as received. Manganese nitrate and zinc nitrate (Fluka Chemicals, Switzerland) were of analytical grade. All aqueous solutions were freshly prepared using ultrapure water from Milli Q plus (Millipore Corp., USA).

### Equipment

The electrosynthesis of nanocomposites was carried out by a potentiostat/galvanostat compactstat (Ivium Technologies, Nethelands). A three-electrode cell was employed during electrosynthesis. The composite 2B pencil graphite (Staedtler Lumograph, Germany) and Pt were respectively used as working and counter electrodes, against pseudo Ag/AgCl reference electrode. The scanning electron microscopy (SEM) model of VEGA Corporation (TESCAN), Czechoslovakia, equipped with energy dispersive X-ray (EDX) using a Leo Supra 50 VP field emission microanalysis system, was used to elucidate the morphology and size of the $Zn_2SiO_4:Mn^{2+}$ nanocomposite. The structure of nanocomposite was determined by FT-IR spectroscopy System 2000 (TENSOR 27, Brucker). The X-ray diffraction (XRD) patterns were recorded with a Philips X-ray diffractometer (Model: PW-2404) employing CuKα radiation at a scanning speed of 2°/min. The photoluminescence (PL) excitation/emission spectra were taken on a Hitachi F-4500 spectrofluorimeter.

### Procedure

$Zn_2SiO_4:Mn^{2+}$ nanocomposite was electrosynthesized by sequential cyclic voltammetry and potentiostatic methods respectively in the potential range of -0.8 to 0.0 V and 0.9 V constant potential. In the cyclic voltammetry method, electrosynthesis of $SiO_2$ was performed using 25 ml solution containing 0.1 M $(NH_4)_2SiF_6$ and 0.5 M KCl in the applied potential ranged mentioned, at a scan rate 100 mV $S^{-1}$ and under OFN atmosphere at room temperature. In order to electrosynthesize $Zn_2SiO_4:Mn^{2+}$, $SiO_2$ electrosynthesized in accordance with the previous method was immersed into 25 ml solution of 0.1 M zinc nitrate containing 0.01 M manganese nitrate, 1 M potassium fluoride and 0.5 M potassium chloride for five minutes in a 0.9 V constant potential.

In this method, the graphite electrode was used as the working electrode, platinum was employed as a counter electrode, and an Ag/AgCl electrode was utilized as the reference electrode.

## RESULTS AND DISCUSSION

### Nanoelectrosynthesis

For nanoelectrosynthesis of $Zn_2SiO_4:Mn^{2+}$, first $SiO_2$ was prepared according to the experimental procedure presented above. Figure 1 indicates the cyclic voltammogram of the formation of $SiO_2$ on the composite graphite electrode. As can be observed, the pair of anodic and cathodic peaks have been developed at the potentials of -0.23 and -0.51 V respectively, which could respectively be attributed to the formation and adsorption of $SiO_2$ and the reduction of Silica.[20] This could be related to the following electrochemical mechanism [Eqs. (1) and (2)].

$$SiF_6^{2-} + 2O^{2-} \rightarrow SiO_2 + 6F^- \quad \text{(anodic)} \qquad \text{Eq. (1)}$$

$$SiO_2 + 4e^- \rightarrow Si(s) + 2O^{2-} \quad \text{(cathodic)} \qquad \text{Eq. (2)}$$

Thereafter, as already mentioned in the Procedure caption, the graphite electrode – modified with $SiO_2$ – was placed inside zinc nitrate 0.1 M solution containing manganese nitrate 0.01 M in the presence of supporting electrolytes of potassium fluoride 1 M and potassium chloride 0.5 M at the constant potential of 0.9 V for five minutes.

According to the proposed mechanism [Eqs. (3) and (4)], mentioned below,

$$4KF + 2SiO_2 \rightarrow K_4SiO_4 + SiF_4 \qquad \text{Eq. (3)}$$

$$K_4SiO_4 + 2Zn(NO_3)_2 + Mn(NO_3)_2 \rightarrow Zn_2SiO_4:Mn + 4KNO_3 \qquad \text{Eq. (4)}$$

the nanocomposite $Zn_2SiO_4:Mn^{2+}$ was synthesized on the electrode. With the change in the concentration of manganese nitrate from 0.01 to 0.02, 0.04, 0.06, and 0.08 M, nanocomposites with different luminescence properties can be synthesized.

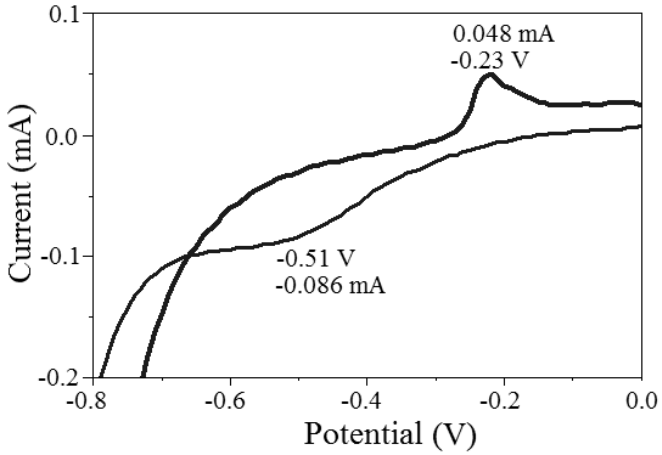


Fig. 1 – The cyclic voltammogram of $SiO_2$ formation starting with $(NH_4)_2SiF_6$ solution containing KCl 0.5 M on the composite graphite electrode. The range of the potential was -0.8–0.0 V with a scan rate of 100 mV/s.

## Energy-dispersive X-ray spectroscopy (EDX) and morphology

To examine the surface morphology of $Zn_2SiO_4:Mn^{2+}$ nanoparticles, scanning electron microscopy (SEM) was employed (Figure 2). The size of the sample particles is around 38.48–120.56 nm. As can be observed in the elemental analysis images obtained, the presence of elements in the nanocomposite is confirmed. The EDX Spectra has been magnified in Fig. 2, so that the presence of manganese becomes evident.

## FT-IR analysis

Figure 3 demonstrates the FT-IR spectrum of the synthesized $Zn_2SiO_4:Mn^{2+}$ nanoparticles. In this spectrum, the 3420 $cm^{-1}$ vibration is related to the symmetrical stretching vibrations ($\upsilon_1$) of the O-H group, which is associated with the water present within the structure of the silicate network. The 521 $cm^{-1}$ peak is associated with the $\upsilon_1$ of Si-O group, while the 1141 and 420 $cm^{-1}$ peaks are respectively related to the asymmetrical stretching vibrations ($\upsilon_3$) of Si-O-Si and the asymmetrical deformation vibrations ($\upsilon_4$) of Si-O group. The vibrational bands of 1020 and 947 $cm^{-1}$ are assigned–to $\upsilon_1$ of $SiO_4$, while the characteristic absorption peaks of 587 $cm^{-1}$ and 683 $cm^{-1}$are respectively caused by $\upsilon_1$ and $\upsilon_3$ of $ZnO_4$.[21-23]

## XRD analysis

Figure 4 indicates the XRD spectrum of manganese-doped $Zn_2SiO_4$ nanoparticles. In this spectrum, some peaks at 2θ angle equal to 25, 32, 34, 38.5, 49.5, and 66 are observed. These are fully congruent with obtained spectra from the nanoparticles prepared by the chemical method[21, 23] and are in accordance with the JCPDS (JCPDS card 37-1485).

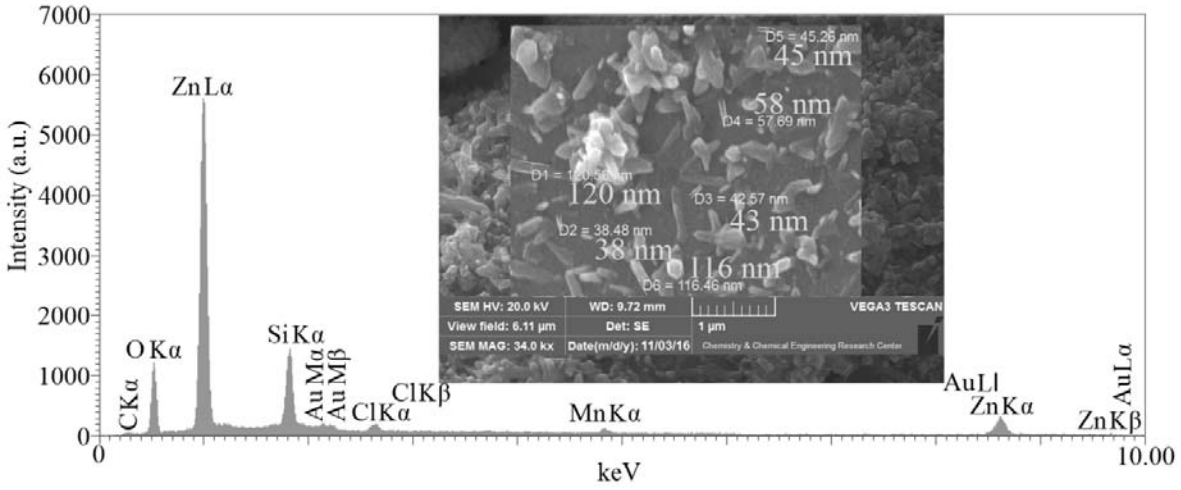


Fig. 2 – EDX spectrum and the electron microscopy image of manganese-doped $Zn_2SiO_4$ nanoparticles.

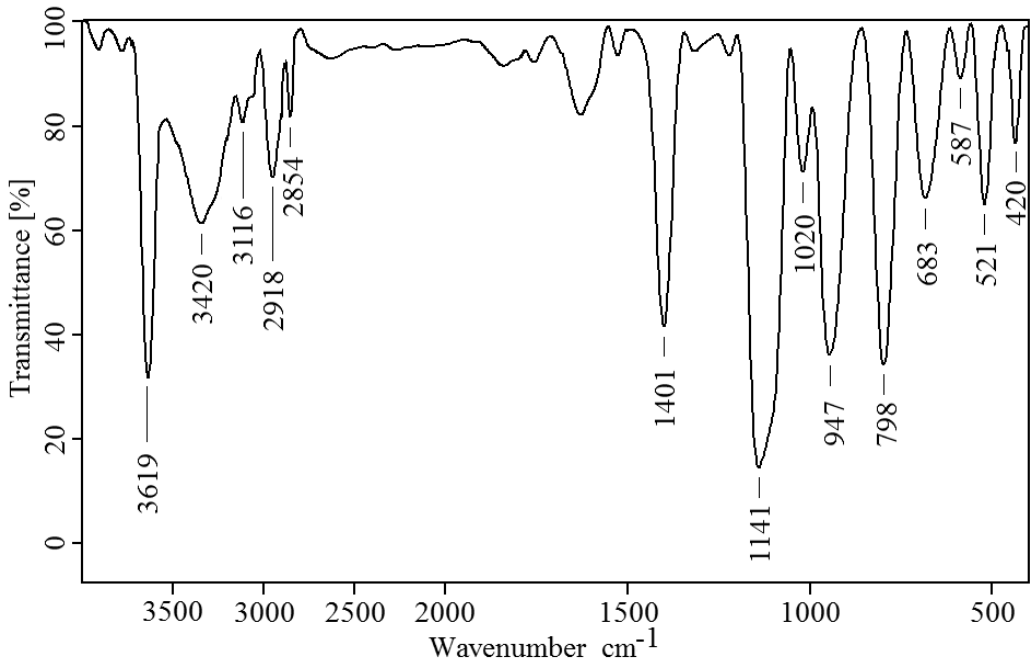


Fig. 3 – The FT-IR spectrum of the synthesized $Zn_2SiO_4$:$Mn^{2+}$ nanoparticles (after smoothing, baseline correction and normalization).

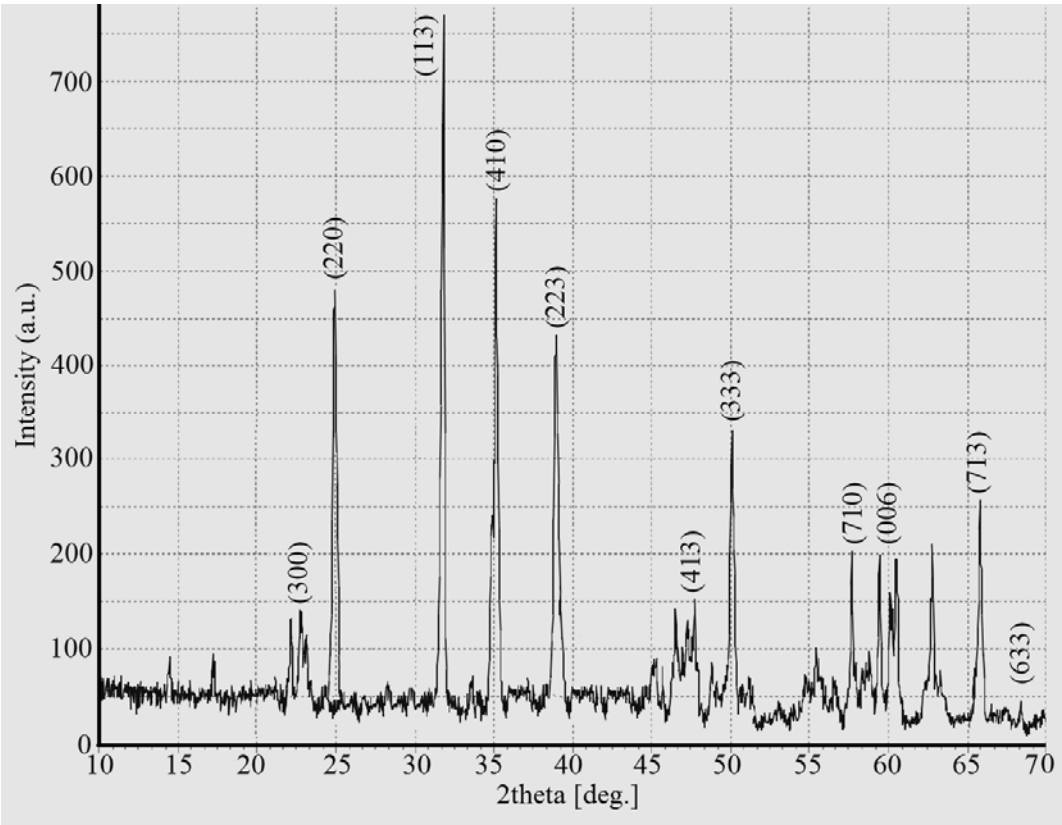


Fig. 4 – The XRD spectrum of manganese-doped $Zn_2SiO_4$ nanoparticles.

The XRD peaks are widened as a result of the nanocrystalline nature of the particles and reduction in the size of particles. These nanocrystals have a lower number of network planes when compared with the bulk substance, which has caused the widening of peaks in the XRD pattern.[24] The average size of crystallites can be determined using the XRD peak widening method. The size of

crystals is calculated through the measurement of the width of the peak in the middle of the highest peak and using the Debye–Scherrer equation. Equation (5) is used in this method to calculate the size of particles:

Lipseste ecuatia (5)

where $D$ is the size of particles in terms of Angstrom, λ is the wavelength of the radiated x-ray, $\beta$ represent the full width at half maximum of the peak with the greatest intensity and $\theta$ denotes the Bragg angle in terms of radiant.[25, 26] The average size of the crystallites calculated by the Debye–Scherrer Equation has been obtained to be within 38.48–120.56 nm (that calculations have been performed in accordance with the specifications of the main peak of the nanocomposite with the intensity of 100%).

## Luminescence properties

Figure 5 indicates the luminescence spectrum of $Zn_2SiO_4:Mn^{2+}$ nanoparticles. In this figure, for the zinc silicate nanoparticles, a reflectance peak is observed within the wavelength of 475–525 nm, indicative of the sparkling green colour of this compound. In the compounds produced by similar methods, this peak too, has been observed.[21, 24] The excitation wavelength of these nanoparticles ranges between 220 and 300 nm with the maximum at 247 nm, as shown in Figure 5.

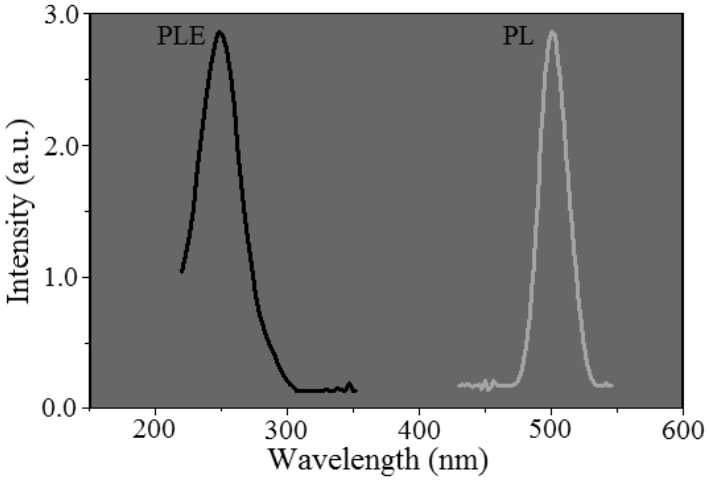


Fig. 5 – The luminescence spectrum of manganese-doped $Zn_2SiO_4$ nanoparticles.

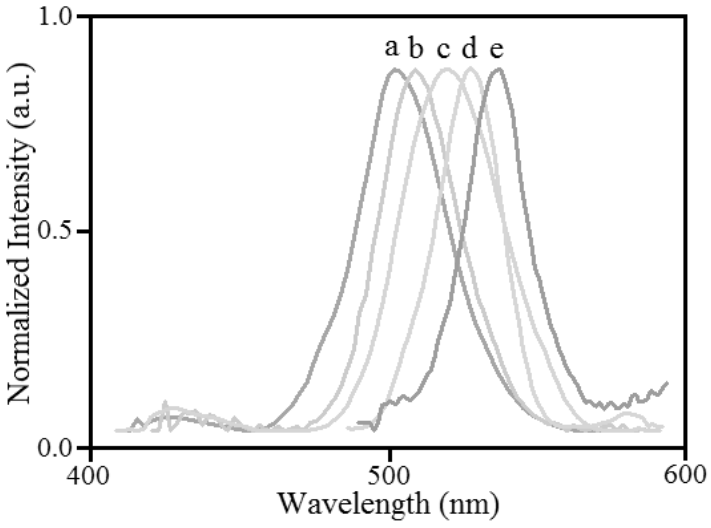


Fig. 6 – The luminescence diagram of zinc silicate particles doped with different concentrations of manganese in the electrosynthesis process. (a–e) Changes in the concentration of manganese nitrate from 0.01 to 0.02, 0.04, 0.06, and 0.08 M, respectively.


Fig. 7 – The cement plasts produced green, red, and blue lights (a) in daylight (b) in darkness using electrosynthesized $Zn_2SiO_4$:Mn nano-particles.

The wavelength of nanocomposites is dependent on the concentration of manganese ions doped in it. The higher the concentration of the manganese doped in the composite, the greater will be the displacement towards the wavelength of red (Figure 6).[24]

The advantage of these nanoparticles over conventional luminescence markers is that even a few hours after being charged with UV light, they can be illuminated by red light to produce green light. This is because when they are charged, electrons are trapped in some levels of energy, after which they can be liberated by lights with a higher wavelength.

### Application of the electrosynthesized nanocomposites

$Zn_2SiO_4:Mn^{2+}$ nanocomposites, which were electrosynthesized, were used in the production of cement plasts (artificial stones). For having the said effects, firstly we need to prepare a suspension made up of $Zn_2SiO_4:Mn^{2+}$ nanocomposites in a specific resin. Then, distribute the resin in mold stones. After half an hour; pour the mortars on the resin. We then put the molds in a shaker for 5 minutes, and at last, after 48 hours, we will have a cement plasts with luminescence properties. Considering the percentage of Mn doped on $Zn_2SiO_4$, the cement plasts produced had radiance towards green and blue lights in darkness (Figure 7).

## CONCLUSION

In this research, manganese-doped zinc silicate was synthesized within nano dimensions by the electrochemical method. With changes in the concentration of manganese in the electrosynthesis of $Zn_2SiO_4:Mn^{2+}$ nanoparticles, the luminescence properties of the nanocomposite were altered in terms of intensity and wavelength of radiation. In this research, manganese-doped $Zn_2SiO_4$ nanoparticles – with suitable optical properties – were used in the fabrication of cement plasts with luminescence properties.

*Acknowledgment:* The authors of the paper sencerely thank the direct financial and spiritual support provided by the head of the University and deputy of research and technology of Islamic Azad University, Yadegar Imam Khomeini Shahre-rey branch.

## REFERENCES

1. Z. Hu, U. Kurien, K. Murwira, A. Ghoshdastidar, O. Nepotchatykh and P. A. Ariya, *ACS Sustain. Chem. Eng.*, **2016**, *4*, 2150-2157.
2. J. P. Wijnen, D. W. J. Klomp, C. I. H. C. Nabuurs, R. A. de Graaf, I. M. L. van Kalleveen, W. J. M. van der Kemp, P. R. Luijten, M. C. Kruit, A. Webb, H. E. Kan and V. O. Boer, *NMR Biomed.*, **2016**, *29*, 1222-1230.
3. R. Cui, D. Xu, X. Xie, Y. Yi, Y. Quan, M. Zhou, J. Gong, Z. Han and G. Zhang, *Food Chem.*, **2017**, *221*, 457-463.
4. Z. Wang, H. Jia, X. Q. Zheng, R. Yang, G. J. Ye, X. H. Chen and P. X. L. Feng, *Nano Lett.*, **2016**, *16*, 5394-5400.
5. M. Nechifor, V. E. Podasca and E. C. Buruiana, *Rev. Roum. Chim.*, **2016**, *4-5*, 363-369.
6. A. Hayat, G. M. Shivashimpi, T. Nishimura, N. Fujikawa, Y. Ogomi, Y. Yamaguchi, S. S. Pandey, T. Ma and S. Hayase, *Appl. Phys. Express*, **2015**, *8*, 047001-047004.
7. M. Sribalaji, P. Arunkumar, K. S. Babu and A. K. Keshri, *Appl. Surf. Sci.*, **2015**, *355*, 112-120.
8. D. Fan, R. Zhang and Y. Li, *Solid State Commun.*, **2010**, *150*, 1911-1914.

9. J. Li, Y. Li, B. Yao, Y. Xu, S. Long, L. Liu, Z. Zhang, L. Zhang, H. Zhao and D. Shen, *J. Chem. Phys.*, **2013**, *138*, 0347041-0347046.
10. H. Cui, Y. Zhou, Z. Gu, H. Zhu, S. Fu and Q. Yao, *Soil Biol. Biochem.*, **2015**, *82*, 119-126.
11. A. P. M. Robertson, C. A. Dyker, P. A. Gray, B. O. Patrick, A. Decken and N. Burford, *J. Am. Chem. Soc.*, **2014**, *136*, 14941-14950.
12. K. Bąk, R. Gaj and A. Budka, *J. Elem.*, **2016**, *21*, 989-999.
13. Y. F. Xue, W. Zhang, D. Y. Liu, H. Y. Xia and C. Q. Zou, *Cereal Chem.*, **2016**, *93*, 543-549.
14. E. Caffau, S. Andrievsky, S. Korotin, L. Origlia, E. Oliva, N. Sanna, H. G. Ludwig and P. Bonifacio, *Astron. Astrophys.*, **2016**, *585*, A16 01-06.
15. D. Ortega, J. C. Hernández-Garrido, C. Blanco-Andujar and J. S. Garitaonandia, *J. Nanopart. Res.*, **2013**, *15*, 2120-2130.
16. A. O. Babatunde, Y. Q. Zhao, A. M. Burke, M. A. Morris and J. P. Hanrahan, *Environ. Pollut.*, **2009**, *157*, 2830-2836.
17. S. Capuani, D. M. Fernandes, J. P. G. Rigon and L. C. Ribeiro, *Commun. Soil Sci. Plant Anal.*, **2015**, *46*, 2901-2912.
18. I. Hosokawa and F. Ohshima, *Water Res.*, **1973**, *7*, 283-289.
19. S. Meis, B. M. Spears, S. C. Maberly, M. B. O'Malley and R. G. Perkins, *J. Environ. Manage.*, **2012**, *93*, 185-193.
20. S. K. Cho, F.-R. F. Fan and A. J. Bard, *Electrochim. Acta*, **2012**, *65*, 57-63.
21. D. Y. Kong, M. Yu, C. K. Lin, X. M. Liu, J. Lin and J. Fang, *J. Electrochem. Soc.*, **2005**, *152*, H146-H151.
22. J. Lin, D. U. Sänger, M. Mennig and K. Bärner, *Mater. Sci. Eng. B*, **1999**, *64*, 73-78.
23. R. P. S. Chakradhar, B. M. Nagabhushana, G. T. Chandrappa, K. P. Ramesh and J. L. Rao, *J. Chem. Phys.*, **2004**, *121*, 10250-10259.
24. Z. T. Kang, Y. Liu, B. K. Wagner, R. Gilstrap, M. Liu and C. J. Summers, *J. Lumin.*, **2006**, *121*, 595-600.
25. Y.-R. Guo, F.-D. Yu, G.-Z. Fang and Q.-J. Pan, *J. Alloys Compd.*, **2013**, *552*, 70-75.
26. H. Shahroosvand and M. Ghorbani-asl, *J. Lumin.*, **2013**, *144*, 223-229.